Journal of Al-Qadisiyah for Computer Science and Mathematics Vol. 15(2) 2023 , pp Math. 65–86

University Of AL-Qadisiyah

Available online at www.qu.edu.iq/journalcm

JOURNAL OF AL-QADISIYAH FOR COMPUTER SCIENCE AND MATHEMATICS

ISSN:2521-3504(online) ISSN:2074-0204(print)

Solving Linear System of Fredholm Integral Equations with Homotopy Analysis and Genetic Algorithms

Rasha F. Ahmed [a,*], ***Waleed Al-Hayani*** [b], ***Abbas Y. Al-Bayati*** [c]

[a]*Department of Mathematics, College of Computer Science and Mathematics, University of Mosul, Mosul, Iraq.*
email: rasha.20csp146@student.uomosul.edu.iq

[b]*Department of Mathematics, College of Computer Science and Mathematics, University of Mosul, Mosul, Iraq.*
emails: waleedalhayani@uomosul.edu.iq, waleedalhayani@yahoo.es

[c]*University of Telafer, Tall'Afar, Iraq.*
email: profabbasalbayati@yahoo.com

ARTICLE INFO

Article history:
Received: 15 /03/2023
Rrevised form: 03 /05/2023
Accepted: 06 /05/2023
Available online: 30 /06/2023

Keywords:

System of Fredholm Integral Equations (SFIEs),

Homotopy Analysis Method (HAM),

h-curves,

Genetic Algorithm (GA).

ABSTRACT

In this paper, we propose a technique called Homotopy Analysis Method (HAM) for solving linear systems of Fredholm integral equations to find relatively close solutions. The HAM approach involves an auxiliary parameter h that offers a straightforward method for adjusting and managing the region where the series of solutions converge. We demonstrate the effectiveness of the HAM approach through our experimental results. Additionally, we improve the HAM approach by incorporating a genetic algorithm (HAM-GA) to further optimize the solutions. The performance of HAM-GA is evaluated by comparing its results to those obtained by HAM, using the residual error function as a fitness function for the genetic algorithm.

https://doi.org/10.29304/jqcm.2023.15.2.1250

1. Introduction

Most often, FIEs result from the mathematical modelling of physical models. FIEs happen in a variety of engineering and physical models, including those that deal with the distribution of polymers in polymeric melts, linear forward modeling, signal processing, etc. Numerous methods for solving FIEs have recently been presented by various writers. Babolian et al. [1] used the technique of decomposition to resolve the second-kind linear FIEs. The decomposition method was put forth by Vahidi and Mokhtari [2] for a second-order linear FIEs system. They

∗Corresponding Author: Rasha F. Ahmed

Email addresses: *rasha.20csp146@student.uomosul.edu.iq*

Communicated by 'sub etitor'

demonstrate that Picard's approach and the method of Adomian decomposition are interchangeable. When using the method of Sinc collocation to achieve a numerical solution to the FIEs, Rashidinia and Zarebnia proved the approximation converges [3]. This method transforms integral system equations into algebraic explicit system equations. Maleknejad et al. [4] introduced the Taylor expansion approach with a weakly or smoothy singular kernel to solve the second FIEs sort. Additionally, Javidi [5] presents the modified homotopy of perturbation technique for finding the system of linear FIEs. A unique multi-parametric homotopy computing technique was introduced by Khan et al. [6]. This was the modified method with three convergence control parameters that create a better homotopy. Muthuvalu and Sulaiman [7] introduced the mean of the half-sweep arithmetic approach using the composite trapezoidal rule to solve FIEs. They look at how well the arithmetic mean approach with a half sweep works for resolving complex linear equations. In mathematical physics solving simultaneous equations of Volterra and Fredholm integral type in two dimensions Khan et al. proposed a discretization technique [8,9]. Additionally, Jafarian and Measoomy [10] employed the feedback neural networks (NNs) method to develop an approximation of the FIEs solution. Taylor expansion has also been suggested for a wide range of methods to solve other types of integral equations [11-13]. Numerous methods according to hyperchaotic behaviours, dynamical systems, and fractional mathematics of Recent developments include a nonautonomous cardiac conduction system [14–23] of specific physical models to find their numerical solutions. The analytical solutions to a set of linear Fredholm equations are presented in this study. A technique known as homotopy analysis can improve the results using the genetic algorithm.

2. Basic Idea of HAM

We shall have a look at the following integral equation to explain the fundamental concepts of the HAM. [24]:

$$\mathrm{N}\left[u(x)\right]=k(x), \tag{1}$$

where $k(x)$ is a standard analytic function, an unknown function, denoted by $u(x)$, x is the independent variable. In addition, $\mathcal{N}$ is a nonlinear operator. By expanding the scope of the conventional homotopy method, Liao [25-28] constructs what is formally known as the equation of zero-order deformation.

$$(1-q)\mathrm{L}\left[\phi(x;q)-u_0(x)\right]=qh\left\{\mathrm{N}\left[\phi(x;q)\right]-k(x)\right\} \tag{2}$$

where h stands for a non-zero auxiliary function, $q \in [0,1]$ represents an embedding parameter, $u_0(x)$ stands for an initial guess of $u(x)$, $\mathcal{L}$ is an operator of auxiliary linear, and $\phi(x;q)$ is an unknown function. It is significant to notice that there is a lot of freedom in choosing auxiliary objects, like $\mathcal{L}$ and h in HAM. [29].

Noticeably, when $q = 0$ and $q = 1$, both

$$\phi(x;0)=u_0(x), \quad and \quad \phi(x;1)=u(x) \tag{3}$$

As q increases from 0 to 1, the solution $\phi(x;q)$ transitions from the initial estimate u_0 (x) to the final solution u(x). This change can be described by expanding $\phi(x;q)$ in a Taylor series with respect to q, yielding the following result: "hold. Thus, the solution $\phi(x;q)$ changes from primary guess $u_0(x)$ to the solution $u(x)$ as q rises from 0 to 1. Expanding $\phi(x;q)$ in Taylor series with respect to q, one has''.

$$\phi(x;q)=u_0(x)+\sum_{m=1}^{+\infty}u_m(x)q^m, \tag{4}$$

$$u_m=\frac{1}{m!}\frac{\partial^m\phi(x;q)}{\partial q^m}\bigg|_{q=0}, \tag{5}$$

If the auxiliary linear, auxiliary function, and auxiliary parameter h operator are all correctly chosen, then, at $q = 1$ and one, series (4) converges, and there is

$$\phi(x;1) = u_0(x) + \sum_{m=1}^{+\infty} u_m(x), \tag{6}$$

This, as demonstrated by Liao [25–28], must be the answer to the equation original nonlinear. If $h = -1$, Equation (3) becomes

$$(1-q)\mathrm{L}\left[\phi(x;q) - u_0(x)\right] + q\left\{\mathrm{N}\left[\phi(x;q)\right] - k(x)\right\} = 0, \tag{7}$$

for which the HPM is mostly utilized [30].

The governing equations, according to (5), is developed from the equations of zeroth-order deformation (2). The vectors are defined as follows

$$\vec{u}_i = \left\{u_0(x), u_1(x), \cdots, u_i(x)\right\}.$$

The equation of mth-order deformation is obtained by differentiating (2), m- times regarding the setting $q = 0$, embedding parameter q, then dividing the results by m!

$$\mathrm{L}\left[u_m(x) - \mathrm{X}_m u_{m-1}(x)\right] = hR_m(u_{m-1}), \tag{8}$$

where

$$R_m(\vec{u}_{m-1}) = \frac{1}{(m-1)!} \frac{\partial^{m-1}\left\{\mathrm{N}\left[\phi(t;q) - k(x)\right]\right\}}{\partial q^{m-1}}\Bigg|_{q=0}, \tag{9}$$

And

$$\mathrm{X}_m = \begin{cases} 1 & m > 1 \\ 0 & m \le 1 \end{cases},$$

In particular, it needs to be said that $u_m(x)$ $(m \geq 1)$ are subject to the original problem's linear equation (9) and conditions of a linear boundary, which are easily resolved by symbolic computation programs like Maple and Matlab.

3. Genetic Algorithm (GA)

A genetic algorithm is a method for improving tough problems and systems of linear equations. Instead of employing deterministic transition rules, GA regulates an alternative population solution identified as iteratively or individually evolving chromosomes. [31]. "Generations" refers to an algorithm's iterations. To replicate how solutions evolve, genetic operators and fitness functions like crossover, mutation, and reproduction are used. [32]. Figure 1 shows a genetic algorithm's initial population, which is often random. A chromosome, which may be either a real number or a binary text, is widely utilized in this population (or mate pool). The objective function, also known as its fitness, assigns a corresponding number to each individual and examines and quantifies a person's performance. The objective function examines It gives each individual a numerical rating based on their performance, known as their fitness. The fittest principle of the survival is implemented after evaluating each chromosome's fitness. In this work, the fitness of each chromosome was assessed by the residual error value. Reproduction, crossover, and mutation are the three main activities carried out by a genetic algorithm. The GA operation sequences are detailed in Figure 1.

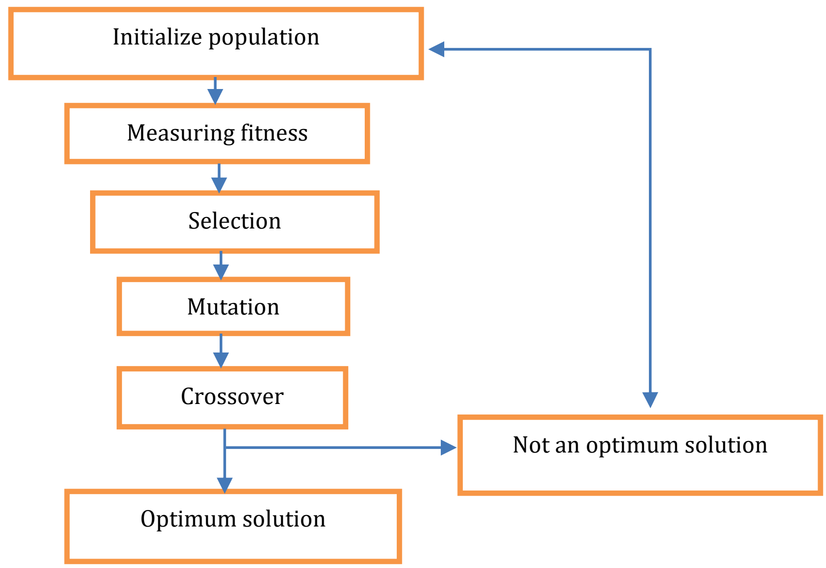

Fig. 1 - Flowchart of genetic algorithm

4. Basic Steps of Genetic Algorithm [33]

Step 1: Initialize each parameter, including the number of clusters, mutation rate, crossover rate, and generations, using a population of random solutions. Identify the coding mode.

Step 2: Determine and assess the fitness function value.

Step 3: To create the new cluster, keep up with the crossover and mutation processes.

Step 4: For the best outcome, Step 2 must be repeated.

Here, we apply the genetic algorithm to enhance the HAM's performance in the following areas:

Table 1 - Genetic Algorithm for the best parameters h and λ_1, λ_2 in system of volterra integral equations

Input:
Set number of variables (var)
Set upper and lower limit for each variable (ub, lb)
Set population size (a),
Set crossover rate (rc)
Set mutation rate (rm)
Set number of iterations (Max_iteration)
Set the name of fitness function
Output:
solution $\boldsymbol{\lambda_1}, \boldsymbol{\lambda_2}$ and $\boldsymbol{h}$
Initialization
1- Generate individual feasible solutions randomly with a limit boundary.
2- Save them in the population p;

3- Find fitness values for each population F
Loop till the terminal condition
4- for $i = 1$ to Max_iteration do
using Rank selection, Elitism based selection
5- fitness = Sort individual descending to find minimum fitness value.
6- Select the best rc solutions in pop1 and save them in popt according to fitness;
Crossover
7- number of crossover nc = (α− ne)/2
8- for j = 1 to nc do
9- arbitrarily choose two solutions XA and XB from Popi;
10- by Arithmetic crossover to XA and XB, produce XC and XD;
11- save XC and XD to popt;
12- endfor
Mutation
13- for j = 1 to ne do
14- select a solution Xj from popt;
15- mutate Random Resetting of Xj under the rate rm and make a new solution Xj';
16- if Xj' is impractical
17- by repairing Xj', renew Xj' with a feasible solution;
18- endif
18- update Xj with Xj' in popt;
19 – endfor
Updating
20- update pop i+1= Pop i + popt;
21- endfor
Returning the best solution
22- put back the best solution X in Pop.

5. Implementations and numerical outcomes

The following three problems in this part show how the HAM was used to get an approximate-exact solution for LSFIEs. The absolute errors ($AE_i, i = 1,2$) between the standard HAM and the HAM developed by the genetic algorithm (HAM-GA) with the exact solutions within the interval $0 \leq x \leq 1$ for $\lambda_i, i = 1,2$ and the various values for h, which are used to demonstrate how accurately the solution results compare to the precise answer, are defined as follows:

$$AE_1 = \left|u_{Exacti}(x_i) - (HAM - GA)\right| \text{ at } h = -1.$$

$$AE_2 = \left|u_{Exacti}(x_i) - (HAM - GA)\right| \text{at } h_1 \text{and } h_2.$$

The Maple 18 package was used to execute the calculations necessary to solve the issues with a 20-digit precision.

5.1. Problem

Let's first consider the following LSFIEs [34]

$$\begin{cases} u_1(x) = f_1(x) + \lambda_1 \int_0^1 \left[x u_1(t) + (x-t) u_2(t) \right] dt, \\ u_2(x) = f_2(x) + \lambda_2 \int_0^1 \left[(x-t) u_1(t) + t u_2(t) \right] dt, \end{cases} \tag{10}$$

$0 \le x \le 1$, where

$$\begin{aligned} f_1(x) &= 2x + \left(-2x + \frac{3}{4} \right) \lambda_1, \\ f_2(x) &= 3x^2 - \left(x + \frac{1}{12} \right) \lambda_2, \end{aligned} \tag{11}$$

with the exact solutions

$$u_{Exact1}(x) = 2x, \quad u_{Exact2}(x) = 3x^2. \tag{12}$$

We select the initial approximation to solve (10) using the standard HAM.

$$u_{1,0}(x) = f_1(x), \quad u_{2,0}(x) = f_2(x) \tag{13}$$

and the linear operator

$$L\left[\phi_1(x,q)\right] = \phi_1(x,q), \quad L\left[\phi_2(x,q)\right] = \phi_2(x,q). \tag{14}$$

Furthermore, the non-linear operator is suggested by the system (10) to be

$$\begin{aligned} &N_1\left[\phi_1(x,q), \phi_2(x,q)\right] = \phi_1(x,q) - f_1(x) \\ &\quad -\lambda_1 \int_0^1 \left[(x+t)\phi_1(t,q) + \left(x + 2t^2\right) \phi_2(t,q) \right] dt, \\ &N_2\left[\phi_1(x,q), \phi_2(x,q)\right] = \phi_2(x,q) - f_2(x) \\ &\qquad -\lambda_2 \int_0^1 \left[x t^2 \phi_1(t,q) + x^2 t \phi_2(t,q) \right] dt, \end{aligned} \tag{15}$$

We create the equation of zeroth-order deformation using the aforementioned formulation, as in (3) and (4), for $m \ge 1$, the equation of *mth*-order deformation is

$$\begin{aligned} L\left[u_{1,m}(x) - \chi_m u_{1,m-1}(x)\right] &= h\left[R_{1,m}\left(\vec{u}_{1,m-1}\right), R_{2,m}\left(\vec{u}_{2,m-1}\right)\right], \\ L\left[u_{2,m}(x) - \chi_m u_{2,m-1}(x)\right] &= h\left[R_{1,m}\left(\vec{u}_{1,m-1}\right), R_{2,m}\left(\vec{u}_{2,m-1}\right)\right], \end{aligned} \tag{16}$$

where

$$\begin{aligned} &R_{1,m}\left(\vec{u}_{1,m-1}, \ \vec{u}_{2,m-1}\right) = u_{1,m-1}(x) - f_1(x) \\ &-\lambda_1 \int_0^1 \left[(x+t) u_{1,m-1}(t) + \left(x + 2t^2\right) u_{2,m-1}(t) \right] dt, \\ &R_{2,m}\left(\vec{u}_{1,m-1}, \ \vec{u}_{2,m-1}\right) = u_{2,m-1}(x) - f_2(x) \\ &\qquad -\lambda_2 \int_0^1 \left[x t^2 u_{1,m-1}(t) + x^2 t u_{2,m-1}(t) \right] dt. \end{aligned} \tag{17}$$

Now, for $m \ge 1$, the solutions of *mth*-order deformation, Equation (17) are

$$u_{1,m}(x) = \chi_m u_{1,m-1}(x) + h\left[R_{1,m}(\vec{u}_{1,m-1}), R_{2,m}(\vec{u}_{2,m-1})\right],$$
$$u_{2,m}(x) = \chi_m u_{2,m-1}(x) + h\left[R_{1,m}(\vec{u}_{1,m-1}), R_{2,m}(\vec{u}_{2,m-1})\right]. \tag{18}$$

In a series form, this results in the approximate answer being given by

$$u_1(x) = u_{1,0}(x) + \sum_{i=1}^{4} u_{1,i}(x), \quad u_2(x) = u_{2,0}(x) + \sum_{i=1}^{4} u_{2,i}(x),$$

This series has the closed form as $m \to \infty$

$$u_1(x) = x, \quad u_2(x) = x^2.$$

which are the exact solutions to the problem (5.1).

Table 1 shows a comparison of the HAM's numerical outcomes standard ($m = 4$), the numerical results of applying the HAM developed by genetic algorithm ($m = 4$) within the interval $0 \le x \le 1$ for $\lambda_1 = 0.16720495, \lambda_2 = 0.1$ and the various values for h, with the exact solution (12). Table 2 displays the absolute errors on the interval h-curves $[-1.2, -0.9]$ when $\lambda_1 = 0.16720495, \lambda_2 = 0.2$.

Table 1 -Numerical results for Problem 5.1

x	i	$u_{Exacti}(x)$	HAM-GA $h = -1$	AE_1	HAM-GA $h_1 = -1.03876$ $h_2 = -1.04018$	AE_2
0.1	1	0.200000000	0.200045760	4.576E-05	0.200000003	3.847E-09
	2	0.030000000	0.029957260	4.273E-05	0.029999770	2.295E-07
0.3	1	0.600000000	0.60002626	2.626E-05	0.599999756	2.433E-07
	2	0.270000000	0.269959552	4.044E-05	0.270000213	2.135E-07
0.5	1	1.000000000	1.000006763	6.763E-06	0.999999509	4.904E-07
	2	0.750000000	0.749961844	3.815E-05	0.750000656	6.567E-07
0.7	1	1.400000000	1.399987265	1.273E-05	1.399999262	7.376E-07
	2	1.470000000	1.469964136	3.582E-05	1.470001099	1.099E-06
0.9	1	1.800000000	1.799967766	3.223E-05	1.799999015	9.848E-07
	2	2.430000000	2.429966428	3.353E-05	2.430001543	1.543E-06

Table 2 **- Absolute errors on the interval *h*-curves for Problem 5.1**

x	$h = -1.2$	$h_1 = -1.03876$ $h_2 = -1.04018$	$h = -1$	$h = -0.9$
0.1	1.324E-04	6.991E-09	4.576E-05	5.710E-04
	1.520E-04	2.330E-07	4.273E-05	3.738E-04
0.3	1.635E-04	2.410E-07	2.626E-05	2.644E-04
	4.438E-05	2.109E-07	4.044E-05	4.642E-04
0.5	1.946E-04	4.891E-07	6.763E-06	4.205E-05
	6.327E-05	6.550E-07	3.815E-05	5.546E-04
0.7	2.257E-04	7.372E-07	1.273E-05	3.485E-04
	1.709E-04	1.099E-06	3.586E-05	6.449E-04
0.9	2.567E-04	9.853E-07	3.223E-05	3.485E-04
	2.785E-04	1.543E-06	3.357E-05	7.353E-04

In Figures 2 and 3, an illustration shows how well the exact solution matches with the approximate solution using the genetic algorithm $h_1 = -1.03876, h_2 = -1.04018$ with $\lambda_1 = 0.16720, \lambda_2 = 0.2$. In Figures 4 and 5, the h-curves present for (problem 5.1) when $\lambda_1 = 0.16720, \lambda_2 = 0.2$.

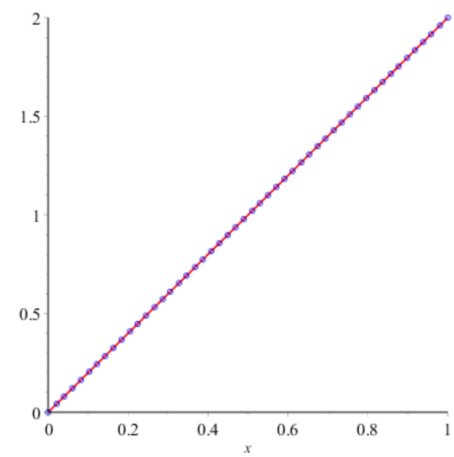

Fig. 2 - $\boldsymbol{Line}: \boldsymbol{u_{Exact1}(x)},\ \boldsymbol{o}: \boldsymbol{HAM - GA_1(x)}$

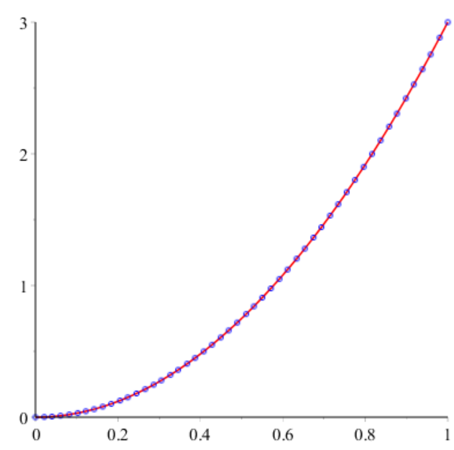

Fig. 3 **-** $\boldsymbol{Line}: \boldsymbol{u_{Exact2}(x)},\ \boldsymbol{o}: \boldsymbol{HAM - GA_2(x)}$

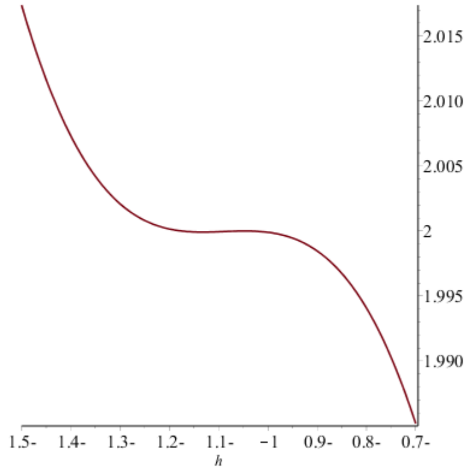

Fig. 4 - h-curve for $u_1'(0.5, h)$

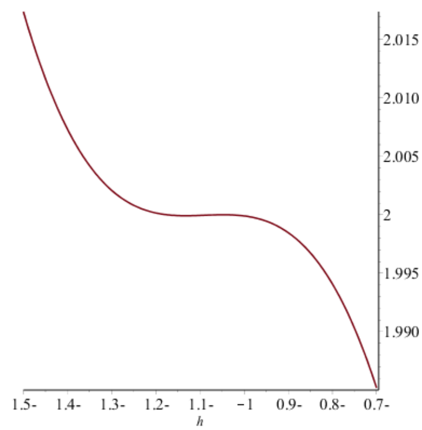

Fig. 5 - h-curve for $u_2'(0.5, h)$

5.2. Problem

Let us now consider the following LSFIEs [34]

$$\begin{cases} u_1(x) = f_1(x) + \lambda_1 \int_0^1 \left[\frac{1}{3}(x+t)\big(u_1(t)+u_2(t)\big) \right] dt, \\ u_2(x) = f_2(x) + \lambda_2 \int_0^1 \left[xt\big(u_1(t)+u_2(t)\big) \right] dt, \end{cases} \tag{19}$$

$0 \le x \le 1,$ where

$$f_1(x) = x + 1 - \left(\frac{17}{18} x + \frac{19}{36} \right) \lambda_1, \qquad f_2(x) = x^2 + 1 - \frac{19}{12} x \lambda_2, \tag{20}$$

with the precise results

$$u_{Exact1}(x) = x + 1, \quad u_{Exact2}(x) = x^2 + 1. \tag{21}$$

We select the initial approximation to solve (19) using the conventional HAM.

$$u_{1,0}(x) = f_1(x), \quad u_{2,0}(x) = f_2(x) \tag{22}$$

and the linear operator

$$L[\phi_1(x,q)] = \phi_1(x,q), \quad L[\phi_2(x,q)] = \phi_2(x,q). \tag{23}$$

Furthermore, the non-linear operator is suggested to be defined as by the system (19) as

$$\begin{aligned} N_1[\phi_1(x,q),\phi_2(x,q)] &= \phi_1(x,q) - f_1(x) \\ &\quad -\lambda_1 \int_0^1 [x\phi_1(t,q) + (x-t)\phi_2(t,q)]dt, \\ N_2[\phi_1(x,q),\phi_2(x,q)] &= \phi_2(x,q) - f_2(x) \\ &\quad -\lambda_2 \int_0^1 [(x-t)\phi_1(t,q) + t\phi_2(t,q)]dt, \end{aligned} \tag{24}$$

We create the equation of zeroth-order deformation like in (2) and (3) using the aforementioned formulation (4) and for $m \geq 1$, the equation of *mth*-order deformation is

$$\begin{aligned} L[u_{1,m}(x) - \chi_m u_{1,m-1}(x)] &= h[R_{1,m}(\vec{u}_{1,m-1}), R_{2,m}(\vec{u}_{2,m-1})], \\ L[u_{2,m}(x) - \chi_m u_{2,m-1}(x)] &= h[R_{1,m}(\vec{u}_{1,m-1}), R_{2,m}(\vec{u}_{2,m-1})], \end{aligned} \tag{25}$$

where

$$\begin{aligned} R_{1,m}(\vec{u}_{1,m-1}, \vec{u}_{2,m-1}) &= u_{1,m-1}(x) - f_1(x) \\ &\quad -\lambda_1 \int_0^1 [xu_{1,m-1}(t) + (x-t)u_{2,m-1}(t)]dt, \\ R_{2,m}(\vec{u}_{1,m-1}, \vec{u}_{2,m-1}) &= u_{2,m-1}(x) - f_2(x) \\ &\quad -\lambda_2 \int_0^1 [(x-t)u_{1,m-1}(t) + tu_{2,m-1}(t)]dt. \end{aligned} \tag{26}$$

Now, for $m \geq 1$, the *mth*-order deformation Equation (26) solutions are

$$\begin{aligned} u_{1,m}(x) &= \chi_m u_{1,m-1}(x) + h[R_{1,m}(\vec{u}_{1,m-1}), R_{2,m}(\vec{u}_{2,m-1})], \\ u_{2,m}(x) &= \chi_m u_{2,m-1}(x) + h[R_{1,m}(\vec{u}_{1,m-1}), R_{2,m}(\vec{u}_{2,m-1})]. \end{aligned} \tag{27}$$

Therefore, the formula for the approximate answer in series form is

$$u_1(x) = u_{1,0}(x) + \sum_{i=1}^{5} u_{1,i}(x), \quad u_2(x) = u_{2,0}(x) + \sum_{i=1}^{5} u_{2,i}(x).$$

This series has the closed form as $m \to \infty$

$$u_1(x) = x+1, \quad u_2(x) = x^2+1.$$

which are the correct answers to the problem (5.2).

Table 3 compares the numerical outcomes obtained using the HAM standard ($m = 5$), the numerical outcomes using the HAM developed by genetic algorithm ($m = 5$) within the interval $0 \leq x \leq 1$ for $\lambda_1 = -0.1$, $\lambda_2 = 0.1$ and the various values for h, with the exact solution (21). Table 4 displays the absolute errors on the interval h-curves $[-1.2, -0.9]$ when $\lambda_1 = 0.16720$, $\lambda_2 = 0.2$.

Table 3 -Numerical results for Problem 5.2

x	i	$u_{Exacti}(x)$	HAM-GA $h=-1$	AE_1	HAM-GA $h_1=-0.99809$ $h_2=-1.00109$	AE_2
0.1	1	1.100000000	1.100000000	5.334E-10	1.100000000	4.806E-10
	2	1.010000000	1.009999999	1.357E-10	1.009999999	1.679E-10
0.3	1	1.300000000	1.100000000	6.953E-10	1.300000000	5.783E-10
	2	1.090000000	1.089999999	4.072E-10	1.089999999	5.038E-10
0.5	1	1.500000000	1.500000000	8.573E-10	1.500000000	6.760E-10
	2	1.250000000	1.249999999	6.787E-10	1.249999999	8.397E-10
0.7	1	1.700000000	1.700000001	1.019E-09	1.700000000	7.737E-10
	2	1.490000000	1.489999999	9.502E-10	1.489999999	1.175E-09
0.9	1	1.900000000	1.900000001	1.181E-09	1.900000000	8.714E-10
	2	1.810000000	1.809999998	1.221E-09	1.809999998	1.511E-09

Table 4 - Absolute errors on the interval *h*-curves for Problem 5.2

x	$h=-1.2$	$h_1=-0.99809$ $h_2=-1.00109$	$h=-1$	$h=-0.9$
0.1	1.107E-04	4.806E-10	5.334E-10	9.430E-05
	2.780E-05	1.679E-10	1.357E-10	2.425E-05
0.3	1.469E-04	5.783E-10	6.953E-10	1.212E-04
	8.340E-05	5.038E-10	4.072E-10	7.275E-05
0.5	1.831E-04	6.760E-10	8.573E-10	1.481E-04
	1.390E-04	8.397E-10	6.787E-10	1.212E-04
0.7	2.192E-04	7.737E-10	1.019E-09	1.750E-04
	1.946E-04	9.068E-10	9.502E-10	1.697E-04
0.9	2.554E-04	8.714E-10	1.181E-09	2.020E-04
	2.502E-04	1.511E-09	1.221E-09	2.182E-04

In Figures 6 and 7, an illustration shows how well the exact solution matches with the approximate solution using the genetic algorithm $h_1=-0.99809, h_2=-1.00109$ with $\lambda_1=-0.1, \lambda_2=0.1$. In Figures 8 and 9 present the h-curves for (problem 5.2).

when $\lambda_1=-0.1, \lambda_2=0.1$.

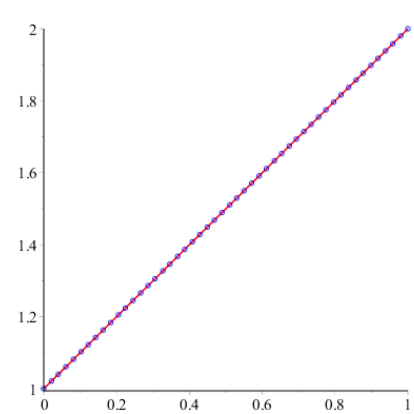

Fig. 6 - ***Line***: $\boldsymbol{u_{Exact1}(x)}$, ***o***: $\boldsymbol{HAM-GA_1(x)}$

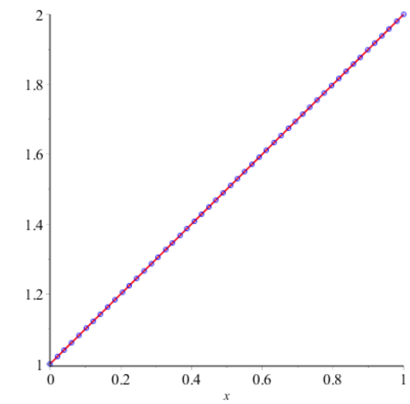

Fig. 7 - $Line$: $u_{Exact2}(x)$, o: $HAM - GA_2(x)$

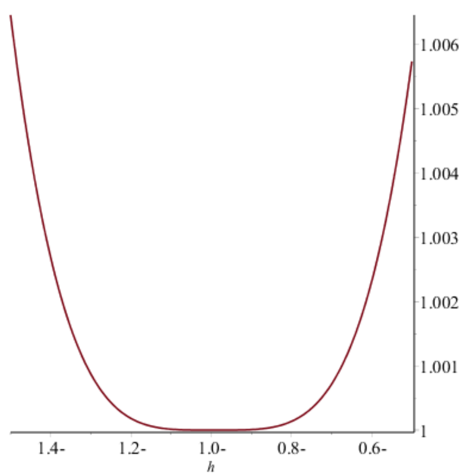

Fig. 8 - h-curve for $u_1'(0.5, h)$

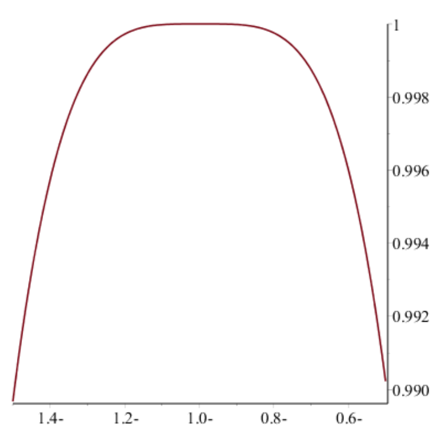

Fig. 9 - h-curve for $u_2'(0.5, h)$

5.3. Problem 5.3

Let's now consider the following LSFIEs [35]

$$\begin{cases} u_1(x) = f_1(x) + \lambda_1 \int_0^1 \left[\left(x^3 + 2t\right) u_1(t) + t^2 u_2(t) \right] dt, \\ u_2(x) = f_2(x) + \lambda_2 \int_0^1 \left[x^2 u_1(t) + \left(x - t^2\right) u_2(t) \right] dt, \end{cases} \tag{28}$$

$0 \le x \le 1,$ where

$$\begin{aligned} f_1(x) &= x^2 + 1 - \left(\frac{4}{3} x^3 + \frac{23}{14} \right) \lambda_1, \\ f_2(x) &= x^4 - \left(\frac{4}{3} x^2 + \frac{1}{5} x - \frac{1}{7} \right) \lambda_2, \end{aligned} \tag{29}$$

with the exact solutions

$$u_{Exact1}(x) = x^2 + 1, \quad u_{Exact2}(x) = x^4. \tag{30}$$

We select the initial approximation to solve (28) using the conventional HAM.

$$u_{1,0}(x) = f_1(x), \quad u_{2,0}(x) = f_2(x) \tag{31}$$

and the linear operator

$$L\left[\phi_1(x,q)\right] = \phi_1(x,q), \quad L\left[\phi_2(x,q)\right] = \phi_2(x,q). \tag{32}$$

Furthermore, the system (28) proposes that the non-linear operator is defined as

$$\begin{aligned} N_1\left[\phi_1(x,q), \phi_2(x,q)\right] &= \phi_1(x,q) - f_1(x) \\ &\quad - \lambda_1 \int_0^1 \left[\left(x^3 + 2t\right) \phi_1(t,q) + t^2 \phi_2(t,q) \right] dt, \\ N_2\left[\phi_1(x,q), \phi_2(x,q)\right] &= \phi_2(x,q) - f_2(x) \\ &\quad - \lambda_2 \int_0^1 \left[x^2 \phi_1(t,q) + \left(x - t^2\right) \phi_2(t,q) \right] dt, \end{aligned} \tag{33}$$

We create the equation of zeroth-order deformation as in (2) and (3) using the above-mentioned formulation (4) and the equation of *mth*-order deformation for $m \ge 1$ is

$$\begin{aligned} L\left[u_{1,m}(x) - \chi_m u_{1,m-1}(x)\right] &= h\left[R_{1,m}\left(\vec{u}_{1,m-1}\right), R_{2,m}\left(\vec{u}_{2,m-1}\right)\right], \\ L\left[u_{2,m}(x) - \chi_m u_{2,m-1}(x)\right] &= h\left[R_{1,m}\left(\vec{u}_{1,m-1}\right), R_{2,m}\left(\vec{u}_{2,m-1}\right)\right], \end{aligned} \tag{34}$$

where

$$R_{1,m}\left(\vec{u}_{1,m-1},\vec{u}_{2,m-1}\right)=u_{1,m-1}(x)-f_1(x)$$
$$-\lambda_1\int_0^1\left[\left(x^3+2t\right)u_{1,m-1}(t)+t^2u_{2,m-1}(t)\right]dt,$$
$$R_{2,m}\left(\vec{u}_{1,m-1},\vec{u}_{2,m-1}\right)=u_{2,m-1}(x)-f_2(x)$$
$$-\lambda_2\int_0^1\left[x^2u_{1,m-1}(t)+\left(x-t^2\right)u_{2,m-1}(t)\right]dt. \tag{35}$$

Now, for $m\geq 1$, the mth-order deformation Equation (35) solutions are

$$u_{1,m}(x)=\chi_m u_{1,m-1}(x)+h\left[R_{1,m}\left(\vec{u}_{1,m-1}\right),R_{2,m}\left(\vec{u}_{2,m-1}\right)\right],$$
$$u_{2,m}(x)=\chi_m u_{2,m-1}(x)+h\left[R_{1,m}\left(\vec{u}_{1,m-1}\right),R_{2,m}\left(\vec{u}_{2,m-1}\right)\right]. \tag{36}$$

Therefore, the formula for the approximate answer in series form is

$$u_1(x)=u_{1,0}(x)+\sum_{i=1}^{5}u_{1,i}(x),\quad u_2(x)=u_{2,0}(x)+\sum_{i=1}^{5}u_{2,i}(x).$$

This series has the closed form as $m\to\infty$

$$u_1(x)=x^2+1,\quad u_2(x)=x^4.$$

which are the exact solutions to the problem (5.3).

Table 5 compares the numerical outcomes obtained using the HAM standard ($m=5$), the numerical outcomes applying the HAM developed by genetic algorithm ($m=5$) within the interval $0\leq x\leq 1$ for $\lambda_1=\lambda_2=0.1$ and the various values for h, with the exact solution (30). Table 6 displays the absolute errors on the interval h-curves $[-1.6,-0.8]$ when $\lambda_1=\lambda_2=0.1$.

Table 5 -Numerical results for Problem 5.3

x	i	$u_{Exacti}(x)$	HAM-GA $h=-1$	AE_1	HAM-GA $h_1=-1.14902$ $h_2=-1.11288$	AE_2
0.1	1	1.010000000	1.009919328	8.067E-05	1.009999662	3.379E-07
	2	0.000100000	0.000106980	6.980E-06	0.000099941	5.804E-08
0.3	1	1.090000000	1.089917635	8.236E-05	1.089999662	3.377E-07
	2	0.008100000	0.008099184	8.150E-07	0.008100027	2.708E-08
0.5	1	1.250000000	1.249911254	8.874E-05	1.249999662	3.372E-07
	2	0.062500000	0.062486179	1.382E-05	0.062500036	3.666E-08
0.7	1	1.490000000	1.489897058	1.029E-04	1.489999663	3.361E-07
	2	0.240100000	0.240067965	3.203E-05	0.240099970	2.929E-08
0.9	1	1.810000000	1.809871923	1.280E-04	1.809999665	3.340E-07
	2	0.656100000	0.656044541	5.545E-05	0.656099829	1.708E-07

Table 6 - Absolute errors on the interval h-curves for Problem 5.3

x	$h=-1.2$	$h_1=-1.14902$ $h_2=-1.11288$	$h=-1$	$h=-0.9$
0.1	2.830E-03	3.379E-07	8.067E-05	1.704E-03
	1.316E-04	5.799E-08	6.980E-06	1.419E-04
0.3	2.891E-03	3.377E-07	8.236E-05	1.740E-03
	2.259E-04	2.708E-08	8.150E-07	2.149E-05
0.5	3.120E-03	3.372E-07	8.874E-05	1.875E-03
	5.072E-04	3.660E-08	1.382E-05	2.950E-04
0.7	3.630E-03	3.361E-07	1.029E-04	2.175E-03
	9.757E-04	2.943E-08	3.203E-05	6.787E-04
0.9	4.532E-03	3.340E-07	1.280E-04	2.706E-03
	1.631E-03	1.710E-07	5.545E-05	1.172E-03

In Figures 10 and 11 an illustration shows how well the exact solution matches with the approximate solution using the genetic algorithm $h_1=-1.14902, h_2=-1.11288$ with $\lambda_1=\lambda_2=0.1$. In Figures 12 and 13 Present the h-curves for (problem 5.3).

when $\lambda_1=\lambda_2=0.1$.

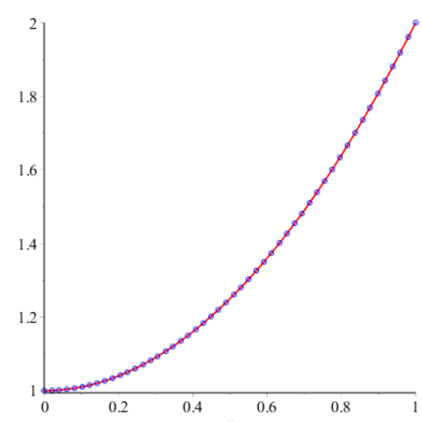

Fig. 10 - *Line*: $u_{Exact1}(x)$, *o*: $HAM-GA_1(x)$

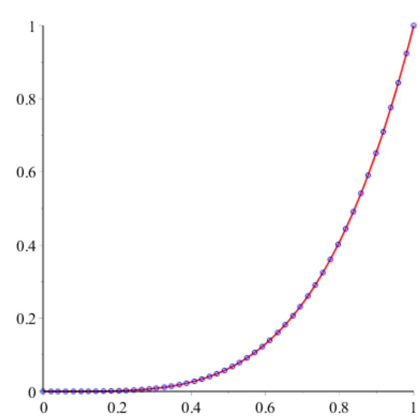

Fig. 11 - *Line*: $u_{Exact2}(x)$, *o*: $HAM-GA_2(x)$

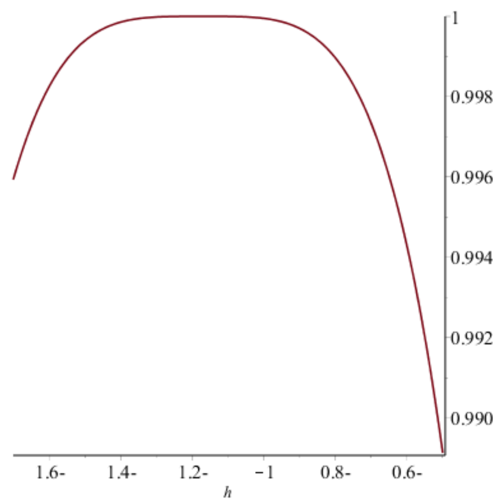

Fig. 12 - h-curve for $u_1'(0.5, h)$

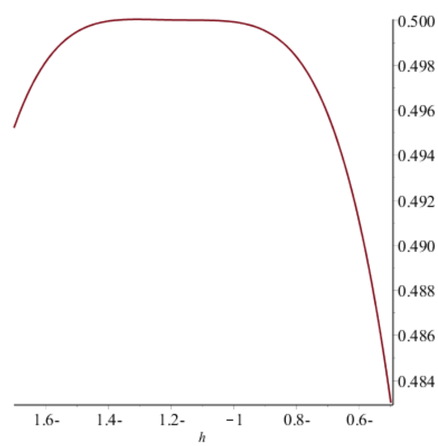

Fig. 13 - h-curve for $u_2'(0.5, h)$

5.4. Problem

Finally, let's now consider the following LSFIEs [35]

$$\begin{cases} u_1(x) = f_1(x) + \lambda_1 \int_0^1 \left[(x-t) u_1(t) + x t u_2(t) \right] dt, \\ u_2(x) = f_2(x) + \lambda_2 \int_0^1 \left[\left(x^2 + 2t \right) u_1(t) + (x+t) u_2(t) \right] dt, \end{cases} \tag{37}$$

$0 \le x \le 1$, where

$$\begin{aligned} & f_1(x) = \left(\sin(1) - \sin(1)x - \cos(1) \right) \lambda_1 + \sin(x), \\ & f_2(x) = \left(\cos(1)x^2 - x^2 - \sin(1)x - 3\sin(1) + \cos(1) + 1 \right) \lambda_2 + \cos(x), \end{aligned} \tag{38}$$

with the exact solutions

$$u_{Exact1}(x) = \sin(x), \quad u_{Exact2}(x) = \cos(x). \tag{39}$$

To solve (37) through the standard HAM, we choose the initial approximation.

$$u_{1,0}(x) = f_1(x), \quad u_{2,0}(x) = f_2(x) \tag{40}$$

and the linear operator

$$L[\phi_1(x,q)] = \phi_1(x,q), \quad L[\phi_2(x,q)] = \phi_2(x,q). \tag{41}$$

Furthermore, the system (37) proposes that the non-linear operator is defined as

$$\begin{aligned} N_1[\phi_1(x,q),\phi_2(x,q)] &= \phi_1(x,q) - f_1(x) \\ &-\lambda_1\int_0^1 [(x-t)\phi_1(t,q) + xt\phi_2(t,q)]dt, \\ N_2[\phi_1(x,q),\phi_2(x,q)] &= \phi_2(x,q) - f_2(x) \\ &-\lambda_2\int_0^1 \left[\left(x^2+2t\right)\phi_1(t,q) + (x+t)\phi_2(t,q)\right]dt, \end{aligned} \tag{42}$$

We create the equation of zeroth-order deformation as in (2) and (3) using the above-mentioned formulation (4) and the equation of *mth*-order deformation for $m \geq 1$ is

$$\begin{aligned} L[u_{1,m}(x) - \chi_m u_{1,m-1}(x)] &= h[R_{1,m}(\vec{u}_{1,m-1}), R_{2,m}(\vec{u}_{2,m-1})], \\ L[u_{2,m}(x) - \chi_m u_{2,m-1}(x)] &= h[R_{1,m}(\vec{u}_{1,m-1}), R_{2,m}(\vec{u}_{2,m-1})], \end{aligned} \tag{43}$$

where

$$\begin{aligned} R_{1,m}(\vec{u}_{1,m-1}, \vec{u}_{2,m-1}) &= u_{1,m-1}(x) - f_1(x) \\ &-\lambda_1\int_0^1 [(x-t)u_{1,m-1}(t) + xtu_{2,m-1}(t)]dt, \\ R_{2,m}(\vec{u}_{1,m-1}, \vec{u}_{2,m-1}) &= u_{2,m-1}(x) - f_2(x) \\ &-\lambda_2\int_0^1 \left[\left(x^2+2t\right)u_{1,m-1}(t) + (x+t)u_{2,m-1}(t)\right]dt. \end{aligned} \tag{44}$$

Now, for $m \geq 1$, the solutions of the *mth*-order deformation Equation (44) are

$$\begin{aligned} u_{1,m}(x) &= \chi_m u_{1,m-1}(x) + h[R_{1,m}(\vec{u}_{1,m-1}), R_{2,m}(\vec{u}_{2,m-1})], \\ u_{2,m}(x) &= \chi_m u_{2,m-1}(x) + h[R_{1,m}(\vec{u}_{1,m-1}), R_{2,m}(\vec{u}_{2,m-1})]. \end{aligned} \tag{45}$$

Therefore, the formula for the approximate solution in series form is

$$u_1(x) = u_{1,0}(x) + \sum_{i=1}^{5} u_{1,i}(x), \quad u_2(x) = u_{2,0}(x) + \sum_{i=1}^{5} u_{2,i}(x).$$

This series has the closed form as $m \to \infty$

$$u_1(x) = \sin(x), \quad u_2(x) = \cos(x).$$

which are the precise answers to the problem (5.4).

Table 7 compares the numerical outcomes obtained using the HAM standard ($m = 5$), the numerical results obtained by applying the HAM developed by genetic algorithm ($m = 5$) within the interval $0 \leq x \leq 1$ for $\lambda_1 = \lambda_2 = 0.1$ and the various values for h, with the exact solution (39). Table 8 displays the absolute errors on the interval h-curves $[-1.6, -0.7]$ when $\lambda_1 = \lambda_2 = 0.1$.

Table 7 -Numerical results for Problem 5.4

x	i	$u_{Exacti}(x)$	HAM-GA $h=-1$	AE_1	HAM-GA $h_1=-1.06915$ $h_2=-1.09388$	AE_2
0.1	1	0.099833416	0.099835597	2.181E-06	0.099834992	1.576E-06
	2	0.995004165	0.994968183	3.598E-05	0.995000841	3.323E-06
0.3	1	0.295520206	0.295516661	3.545E-06	0.295520865	6.589E-07
	2	0.955336489	0.955292268	4.422E-05	0.955333758	2.730E-06
0.5	1	0.479425538	0.479416267	9.271E-06	0.479425280	2.583E-07
	2	0.877582561	0.877529570	5.299E-05	0.877579708	2.853E-06
0.7	1	0.644217687	0.644202689	1.499E-05	0.644216511	1.175E-06
	2	0.764842187	0.764779891	6.229E-05	0.764838495	3.692E-06
0.9	1	0.783326909	0.783306185	2.072E-05	0.783324816	2.092E-06
	2	0.621609968	0.621537835	7.213E-05	0.621604722	5.246E-06

Table 7 - Absolute errors on the interval *h*-curves for Problem 5.4

x	$h=-1.2$	$h_1=-1.06915$ $h_2=-1.09388$	$h=-1$	$h=-0.9$
0.1	2.937E-03	1.576E-06	2.181E-06	2.369E-04
	3.874E-03	3.323E-06	3.598E-05	2.463E-03
0.3	2.253E-03	6.589E-07	3.545E-06	1.491E-04
	3.903E-03	2.730E-06	4.422E-05	3.010E-03
0.5	1.568E-03	2.583E-07	9.271E-06	5.352E-04
	4.407E-03	2.853E-06	5.299E-05	3.604E-03
0.7	8.837E-04	1.175E-06	1.499E-05	9.213E-04
	5.387E-03	3.692E-06	6.229E-05	4.245E-03
0.9	1.991E-04	2.092E-06	2.072E-05	1.307E-03
	6.843E-03	5.246E-06	7.213E-05	4.932E-03

In Figures 14 and 15 An illustration shows how well the exact solution matches with the approximate solution using the genetic algorithm $h_1=-1.06915, h_2=-1.09388$ with $\lambda_1=\lambda_2=0.1$. In Figures 16 and 17 Present the h-curves for (problem 5.4).

when $\lambda_1=\lambda_2=0.1$.

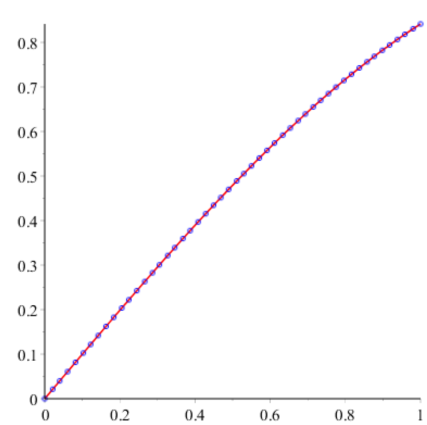

Fig. 14 -*Line*: $u_{Exact1}(x)$, *o*: $HAM-GA_1(x)$

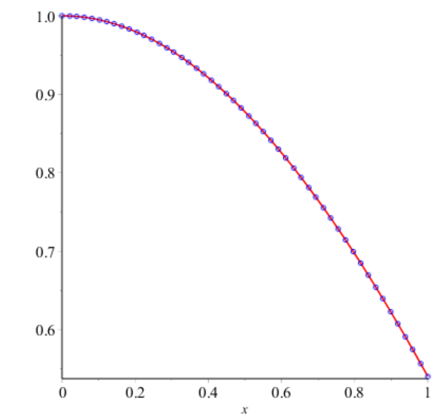

Fig. 15 -*Line*: $u_{Exact1}(x)$, o: $HAM - GA_2(x)$

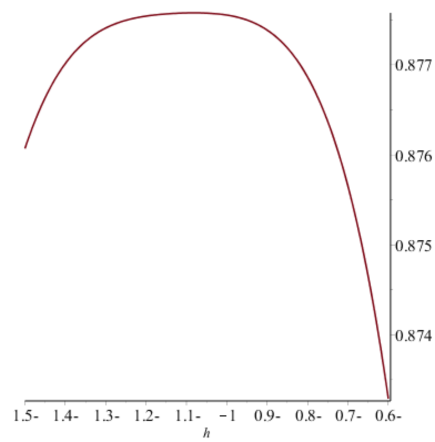

Fig. 16 - h-curve for $u_1'(0.5, h)$

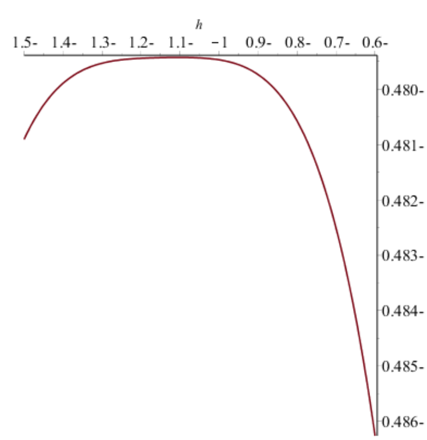

Fig. 17 - h-curve for $u_2'(0.5, h)$

6. Conclusions

The current study proposes a new algorithm (HAM-GA) designed for the linear system equations solving of Fredholm integral by merging the GA and the HAM. The program calculates the answer based on four consecutive cases. The algorithm chooses the best value for λ_1 , λ_2 and h based on the residual error function's classification as a fitness function. In the first instance, the results were determined using the normal HAM, whereas in the second instance, the optimal value for h was selected using the genetic algorithm, and the results were determined using the HAM-GA. Lastly, HAM-GA was used to determine the findings based on optimal λ_1 , λ_2 , and h.

The results achieved with the best h were superior to those produced by the conventional HAM. The fourth case's outcomes were perfect for the precise solution. The results show that the suggested approach is successful in locating the solution because they are in good agreement with the h-curves.

Conflicts of Interest

The authors declares that there is no conflict of interest regarding the publication of this paper.

References

[1] E. Babolian, J. Biazar, and A. Vahidi, "The decomposition method applied to systems of Fredholm integral equations of the second kind," *Applied Mathematics Computation*, vol. 148, no. 2, pp. 443-452, 2004.

[2] A. Vahidi and M. Mokhtari, "On the decomposition method for system of linear Fredholm integral equations of the Second Kind," *J. Appl. Math. Scie*, vol. 2, no. 2, pp. 57-62, 2008.

[3] J. Rashidinia and M. Zarebnia, "Convergence of approximate solution of system of Fredholm integral equations," *Journal of Mathematical Analysis Applications*, vol. 333, no. 2, pp. 1216-1227, 2007.

[4] K. Maleknejad, N. Aghazadeh, and M. Rabbani, "Numerical solution of second kind Fredholm integral equations system by using a Taylor-series expansion method," *Applied Mathematics Computation,* vol. 175, no. 2, pp. 1229-1234, 2006.

[5] M. J. M. Javidi and c. modelling, "Modified homotopy perturbation method for solving system of linear Fredholm integral equations," vol. 50, no. 1-2, pp. 159-165, 2009.

[6] Y. Khan, K. Sayevand, M. Fardi, and M. Ghasemi, "A novel computing multi-parametric homotopy approach for system of linear and nonlinear Fredholm integral equations," *Applied Mathematics Computation,* vol. 249, pp. 229-236, 2014.

[7] M. S. Muthuvalu and J. Sulaiman, "Half-Sweep Arithmetic Mean method with composite trapezoidal scheme for solving linear Fredholm integral equations," *Applied Mathematics Computation,* vol. 217, no. 12, pp. 5442-5448, 2011.

[8] F. Khan, G. Mustafa, M. Omar, and H. Komal, "Numerical approach based on Bernstein polynomials for solving mixed Volterra-Fredholm integral equations," *AIP Advances,* vol. 7, no. 12, p. 125123, 2017.

[9] F. Khan, M. Omar, and Z. Ullah, "Discretization method for the numerical solution of 2D Volterra integral equation based on two-dimensional Bernstein polynomial," *AIP Advances,* vol. 8, no. 12, p. 125209, 2018.

[10] A. Jafarian and S. M. Nia, "Utilizing feed-back neural network approach for solving linear Fredholm integral equations system," *Applied Mathematical Modelling,* vol. 37, no. 7, pp. 5027-5038, 2013.

[11] P. Huabsomboon, B. Novaprateep, and H. Kaneko, "On Taylor-series expansion methods for the second kind integral equations," *Journal of computational applied Mathematics Computation,* vol. 234, no. 5, pp. 1466-1472, 2010.

[12] S. S. Ray and P. Sahu, "Numerical methods for solving Fredholm integral equations of second kind," in *Abstract and Applied Analysis*, 2013, vol. 2013: Hindawi.

[13] K. Maleknejad and A. Arzhang, "Numerical solution of the Fredholm singular integro-differential equation with Cauchy kernel by using Taylor-series expansion and Galerkin method," *Applied Mathematics Computation*, vol. 182, no. 1, pp. 888-897, 2006.

[14] D. Baleanu, A. Jajarmi, H. Mohammadi, and S. Rezapour, "A new study on the mathematical modelling of human liver with Caputo–Fabrizio fractional derivative," *Chaos, Solitons Fractals,* vol. 134, p. 109705, 2020.

[15] A. H. Ali, G. A. Meften, O. Bazighifan, M. Iqbal, S. Elaskar, and J. Awrejcewicz, "A study of continuous dependence and symmetric properties of double diffusive convection: forchheimer model," *Symmetry*, vol. 14, no. 4, p. 682, 2022.

[16] G. A. Meften, A. H. Ali, K. S. Al-Ghafri, J. Awrejcewicz, and O. Bazighifan, "Nonlinear stability and linear instability of double-diffusive convection in a rotating with LTNE effects and symmetric properties: brinkmann-forchheimer model," *Symmetry*, vol. 14, no. 3, p. 565, 2022.

[17] G. A. Meften, A. H. Ali, and M. T. Yaseen, "Continuous dependence for thermal convection in a Forchheimer-Brinkman model with variable viscosity," *AIP Conference Proceedings*, vol. 2457, no. 1, p. 020005, 2022.

[18] T. Omay and D. Baleanu, "Fractional unit-root tests allowing for a fractional frequency flexible Fourier form trend: predictability of Covid-19," *Advances in Difference Equations*, vol. 2021, no. 1, p. 167, 2021.

[19] R. T. Alqahtani, A. Yusuf, and R. P. Agarwal, "Mathematical analysis of oxygen uptake rate in continuous process under caputo derivative," *Mathematics,* vol. 9, no. 6, p. 675, 2021.

[20] D. Baleanu, B. Ghanbari, J. H. Asad, A. Jajarmi, and H. M. Pirouz, "Planar system-masses in an equilateral triangle: numerical study within fractional calculus," *Computer Modeling in Engineering Sciences,* vol. 124, no. 3, pp. 953-968, 2020.

[21] I. Jaradat, M. Alquran, S. Sivasundaram, and D. Baleanu, "Simulating the joint impact of temporal and spatial memory indices via a novel analytical scheme," *Nonlinear Dynamics,* vol. 103, no. 3, pp. 2509-2524, 2021.

[22] N. H. Tuan, D. Baleanu, T. N. Thach, D. O'Regan, and N. H. Can, "Final value problem for nonlinear time fractional reaction–diffusion equation with discrete data," *Journal of Computational Applied Mathematics Computation*, vol. 376, p. 112883, 2020.

[23] S. Qureshi and A. Yusuf, "A new third order convergent numerical solver for continuous dynamical systems," *Journal of King Saud University-Science,* vol. 32, no. 2, pp. 1409-1416, 2020.

[24] A. Georgieva and S. Hristova, "Homotopy analysis method to solve two-dimensional nonlinear Volterra-Fredholm fuzzy integral equations," *Fractal Fractional,* vol. 4, no. 1, p. 9, 2020.

[25] S. Liao, *Beyond perturbation: introduction to the homotopy analysis method*. CRC press, 2003.

[26] S. Liao, "Comparison between the homotopy analysis method and homotopy perturbation method," vol. 169, no. 2, pp. 1186-1194, 2005.

[27] S. Liao, *Homotopy analysis method in nonlinear differential equations*. Springer, 2012.

[28] S. Liao, *Advances in the homotopy analysis method*. World Scientific, 2013.

[29] A. Jafarian, P. Ghaderi, A. K. Golmankhaneh, and D. Baleanu, "Analytical treatment of system of Abel integral equations by homotopy analysis method," *Rom. Rep. Phys,* vol. 66, no. 3, pp. 603-611, 2014.

[30] E. Hetmaniok, D. Słota, T. Trawiński, and R. Wituła, "Usage of the homotopy analysis method for solving the nonlinear and linear integral equations of the second kind," *Numerical Algorithms,* vol. 67, pp. 163-185, 2014.

[31] O. Kramer, *Genetic algorithm essentials* Springer, 2017.

[32] K.-F. Man, K.-S. Tang, and S. Kwong, "Genetic algorithms: concepts and applications [in engineering design]," *IEEE transactions on Industrial Electronics,* vol. 43, no. 5, pp. 519-534, 1996.
[33] A. Jayachitra and R. Vinodha, "Genetic algorithm based PID controller tuning approach for continuous stirred tank reactor," *Advances in Artificial Intelligence,* vol. 2014, pp. 9-9, 2015.
[34] J.-H. He, M. H. Taha, M. A. Ramadan, and G. M. Moatimid, "A combination of bernstein and improved block-pulse functions for solving a system of linear fredholm integral equations," *Mathematical Problems in Engineering,* vol. 2022, pp. 1-12, 2022.
[35] Z. Elahi, S. S. Siddiqi, and G. Akram, "Laguerre method for solving linear system of Fredholm integral equations," *International Journal of Computer Mathematics,* vol. 98, no. 11, pp. 2175-2185, 2021.